ASME Journal of Nondestructive Evaluation, Diagnostics and Prognostics of Engineering Systems
Online journal at:
https://asmedigitalcollection.asme.org/nondestructive

Improving the Signal-to-Noise Ratio of Eddy Current Thickness Gauges Used to Measure Metal Coatings on Moving Test Objects

Volodymyr Ya Halchenko
Department of Instrumentation, Mechatronics and Computerized Technologies,
Cherkasy State Technological University,
460 Shevchenko Blvd.,
18006 Cherkasy, Ukraine
e-mail: v.halchenko@chdtu.edu.ua

Ruslana Trembovetska
Department of Instrumentation, Mechatronics and Computerized Technologies,
Cherkasy State Technological University,
460 Shevchenko Blvd.,
18006 Cherkasy, Ukraine
e-mail: r.trembovetska@chdtu.edu.ua

Volodymyr Tychkov[1]
Department of Instrumentation, Mechatronics and Computerized Technologies,
Cherkasy State Technological University,
460 Shevchenko Blvd.,
18006 Cherkasy, Ukraine
e-mail: v.tychkov@chdtu.edu.ua

The article focuses on the generalized application of the method developed by the authors to improve the signal-to-noise ratio based on Taguchi's robust parameter design to the entire class of surface eddy current thickness gauges for nonmagnetic metal coatings, applied to metal nonferromagnetic and weakly magnetic substrates of moving planar objects, without physically eliminating the effects of noise factors. In the specific examples presented, robust configurations of eddy current probes have been found, namely, their corresponding technical modifications, which are characterized by the maximum possible signal-to-noise ratios and ensure the minimization of the variance of the output signals directly selected from them, which were disturbed by all the uncontrolled noise factors, without additional processing. For robust design, a mathematical model of a probe over a moving object with a coating was used, which, together with the use of orthogonal arrays, allows Taguchi's designs of experiment to be created and implemented. As a result, the obtained data were used to evaluate design options using the "larger is better" quality loss function and the signal-to-noise ratios calculated on its basis, which made it possible to select the optimal combination of design and operating parameters for thickness gauges. The efficiency and reliability of the found optimal configurations of eddy current probes have been proven by confirmatory numerical calculations. A numerical–experimental Monte-Carlo method has demonstrated a significant reduction in the effect of various noises on signals of optimal thickness gauge designs with an evaluation of variations around their undistorted noise variants. Using variance analysis, a hierarchy of the influence on the characteristics of the signals of probes by their design and operating parameters has been established. This made it possible to formulate technical requirements for the accuracy of manufacturing designs and conditions for maintaining the operating modes of probes. [DOI: 10.1115/1.4072169]

Keywords: eddy current measurement of metal coating thickness, moving tested object, weakly magnetic and nonferromagnetic substrates, robust parametric design, Taguchi's design of experiment, signal-to-noise ratio, suppression of uncontrollable noises, materials testing, numerical analysis, product quality control, sensors, testing methodologies

1 Introduction

Due to their mechanical, physical, and decorative properties, coatings made of nonferromagnetic metals and their alloys are widely used in the industry for a variety of functional purposes to apply to conductive products. It is quite common for such products to be made of nonmagnetic metals. In this study, we will focus on planar test objects (TOs) with a characteristic "coating-substrate" two-layer structure in the form of "conductive nonferromagnetic metal coating—conductive nonmagnetic metal substrate," which make up a rather significant part of the total volume of such products. The choice of substrate material is made depending on the requirements for the product in terms of mechanical, physical, and chemical properties and cost. The most common types of substrates for these TO structures are brass, bronze, aluminum, copper, titanium, and stainless steel, but cadmium, copper, aluminum, silver, etc., are also used for coating. Typically, situations arise where the coating and the substrate are characterized by significant differences in electrical conductivity, i.e., either the coating is a better conductor than the substrate or the coating is the worst conductor. In any case, the quality of the finished product also depends on the quality of the coating, which is largely determined by the actual thickness and uniformity of the coating. Consequently, measuring the thickness of coatings

[1]Corresponding author.
Manuscript received January 16, 2026; final manuscript received June 3, 2026; published online July 9, 2026. Assoc. Editor: Henning Heuer.

is of great importance in the nondestructive testing of finished products to ensure their required properties. It should also be noted that in industry, such testing often needs to be performed in conditions where the TO is movable. This causes certain difficulties in the implementation of measurements, which are difficult to overcome with some testing methods.

Among all the methods of nondestructive testing of the thickness of metal coatings on metal substrates, preference is often given to eddy current techniques, which have recently been significantly developed and have received attention from researchers. The primary task in measurements is to ensure that eddy current probes (ECPs) used in testing are insensitive to changes in the lift-off and to noise uncontrollable factors inherent in the TO. They usually include, in the case of the research, local variations in the electrical conductivity of the materials of both the coating and the TO substrate. The final result of such actions is an increase in the signal-to-noise ratio (SNR) of the probes to the maximum available values, since their low values do not allow fixing insignificant signal changes [1].

Possible options for appropriate technical solutions are being worked out by scientists, ranging from fairly simple to complex proposals. The conditionally simple methods include single-frequency methods, for example [2]. Moreover, in Ref. [2], based on the established linear relationship between the tangent of the phase angle of the ECP signal and lift-off, i.e., the phase linear feature introduced by the authors, a new method of thickness measurement based on the fixed lift-off deviation was proposed, but it demonstrates a certain stability against the influence of this interference alone. In studies [2,3], a critical analysis was made of the use of specific techniques for the excitation of eddy currents, in particular, a swept-frequency eddy current (SFEC) [4] and a pulsed eddy current (PEC) [5,6]. The author notes certain advantages of these approaches and, most importantly, emphasizes their disadvantages, i.e., the availability of expensive equipment and more complex technical operations. In particular, the application of SFEC often involves the use of impedance analyzers, and the estimation of measured coating thickness values is based on potentially complex analytical relationships. In turn, the use of PEC for measurements requires advanced signal processing to extract useful information from the pulsed signals. For example, in studies [7,8], the accent for noise suppression is placed on the use of specific computational processing techniques. At the same time, they are not oriented to reduce the negative effect on measurements of such uncontrollable parameters as local variations in the electrophysical properties of the TO material. A similar drawback is also inherent in the approach proposed in Ref. [9].

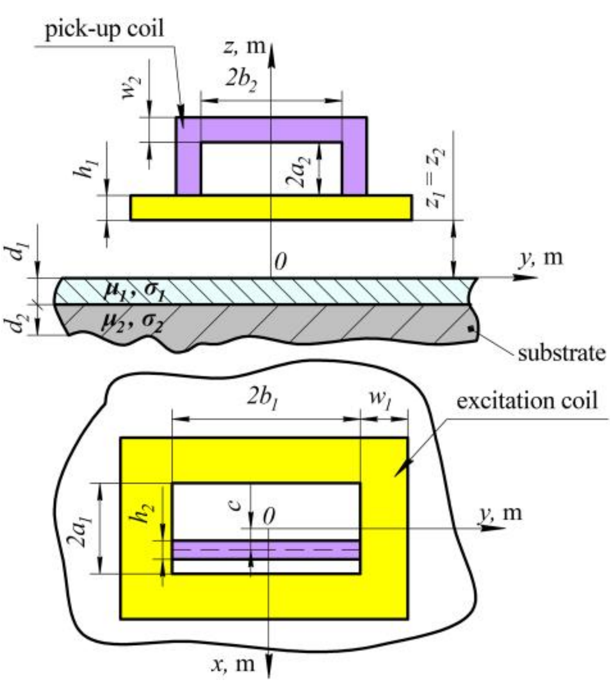

Fig. 1 Geometric model of the eddy current gauge for the thickness coating on a moving test object

Even more problematic is the use of the multifrequency eddy current method [10,11], which is implemented in the frequency domain and also quite often requires the use of such complex and cost-intensive conventional equipment as multifrequency impedance analyzers.

Thus, all of these methods are largely aimed at eliminating or at least reducing the harmful effect of the lift-off on the results of ECP measurements of coating thickness. However, their effect on the interfering factors that are characteristic of TO is only partial and does not lead to a complete elimination. However, although the effect of these interferences on the variations of the ECP signals is much smaller compared to the lift-off, it is still desirable to reduce them, since the local scatter of electrical conductivity for nonferrous metals is from 5% to 10% [12].

References [13–18] are more promising in this regard. They consider the possibilities of using the apparent eddy current conductivity (AECC) spectroscopy method and its certain modifications. The approach involves the use of a rather mathematically complex inversion algorithm based on the AECC curve to estimate the thickness of metal coatings on nonmagnetic metals. This algorithm eliminates the effects of lift-off and coil parameters of the ECP, allowing coating thickness and conductivity to be directly detected by extracting information characteristics from the AECC. Due to the correspondence to the planar wave approximation, the method is characterized by existing problems with the use of rather bulky in size electromagnetic field sources, which also introduce certain limitations in its application.

To improve the metrological performance of eddy current thickness gauges, the improved signals of which are obtained directly from the probes, and optimization of their design using the theory of design of experiment (DOE) was used in Ref. [19]. An effective method for simultaneously increasing the SNR and reducing signal variations in electrical conductivity and magnetic permeability meters to interference is proposed by the authors of the article in publications [20–22]. This problem for probes with a different functionality is solved by finding their optimal designs using the Taguchi robust parameter design method. The positive results of applying the Taguchi optimization method are demonstrated, which are especially convincing for solving the first of the problems. Unfortunately, we could not find any studies by other authors devoted to the problem under consideration using this method. Consequently, we note that generalization of the proposed approach to ECPs for other target applications is promising and appropriate, since the desired result is achieved even when the signal is sampled directly from the probes, even without its preliminary processing.

We emphasize that, unlike the approaches analyzed in the literature review, the method proposed by the authors allows achieving the stated goal without the necessary processing of the selected signal, obtaining it in an informationally improved form directly from an optimally designed meter. This is a significant advantage of the proposed method, which allows obtaining an undistorted signal directly from the meter without performing additional computational procedures during its processing. Noise reduction can be achieved by successfully compromising between the mutual nonlinear complex cross-action of a significant number of factors that determine the output signal level of the probe and its sensitivity to interference at the stage of its formation. The method can be used in combination with other approaches for final noise suppression based on calculations during signal processing and implemented on already selected information.

This article proposes a generalized extension of the method developed by the authors for improving the SNR using Taguchi's robust parametric design to the whole class of surface transformer

Table 1 A set of controllable parameters

Controllable parameters	Variation range
Excitation coil width a_1, m	0.010–0.020
Excitation coil length b_1, m	0.016–0.024
Cross-sectional height of the excitation coil h_1, m	0.004–0.008
Cross-sectional width of the excitation coil w_1, m	0.001–0.004
Pick-up coil width a_2, m	0.003–0.005
Pick-up coil length b_2, m	0.010–0.014
Cross-sectional height of the pick-up coil h_2, m	0.001–0.002
Cross-sectional width of the pick-up coil w_2, m	0.001–0.002
Interaxial distance between the pick-up and excitation coils c, m	0.002–0.009
Moving speed of TO v, m/s	15–25
Excitation frequency f, kHz	1.5–4.5
Excitation current I, A	0.1–0.3

eddy current thickness gauges for nonmagnetic metal coatings applied to nonferromagnetic and weakly magnetic metal substrates. It allows the determination of optimal configurations of probe designs for measuring the thickness of coatings on moving planar objects. The method ensures simultaneous suppression without actually eliminating uncontrollable noise factors, in particular those caused by changes in the lift-off and local variations in electrical conductivity of both the substrate materials of the objects and, most importantly, their coatings.

The remainder of this article is organized as follows: Sec. 2 contains the methods used in the research, including Taguchi's robust parameter design, mathematical model of a coating thickness gauge, Taguchi design of experiments and optimal design, variance ANOVA analysis of ECP parameters; Sec. 3 describes our results; Sec. 4 discusses these results qualitatively and Sec. 5 contains conclusions.

2 Methods

2.1 Taguchi's Robust Parameter Design. The description of the main stages of the algorithm in detail can be found in a number of monographs, in particular [23], including updated modern ones [24,25]. An extended version of the algorithm for designing eddy current probes can be found in the previously mentioned publications [20,21]. We give brief information on the main stages of the Taguchi method, which are necessary for the robust parameter design of the ECP, which are actually the tasks of the study: to select the characteristic of the TO measured by the probe, which is recorded by its output signal; to identify the controllable parameters of the ECP, namely its operating and design parameters, as well as possible levels of their gradation during variation; to determine the noise factors, that are uncontrollable, and their gradation levels; to assign intervals of changes in the controllable and noise factors; to select the orthogonal arrays corresponding to the characteristics of both groups of factors; to create a Taguchi DOE and conduct them, using computer simulation to calculate the output signal of the ECP according to the proposed mathematical model; according to the values of SNR calculated on the basis of the Taguchi quality loss function for each test, select the optimal configuration of the ECP design according to the appropriate combination of gradation levels of controllable factors that maximizes this indicator; to conduct confirmatory numerical experiments to verify the found optimal configuration parameters of the ECP design; to perform analysis of variance (ANOVA) of the influence of controllable factors on the SNR. We will accompany the implementation of all stages of robust parameter design of the ECP with relevant examples in the further course of implementation.

2.2 Mathematical Model of a Coating Thickness Gauge. The optimization of ECP designs by means of the theory of DOE, including the Taguchi method, involves the creation of a plan that contains design options determined by combinations of controllable design and operating parameters of ECPs and the effects of all the interfering factors. For each of these cases, it is necessary to calculate the output signal of the probe. To this aim, let us define the type of ECP, the general view and geometric characteristics of which are illustrated in Fig. 1, which also shows the structure of a two-layer moving TO.

It should be noted that the electrical connection scheme of the ECP pick-up coil is not essential in the context of this research and was not considered. The rectangular design of the ECP coils was chosen due to their ability, by implementing the "uniform eddy current" concept, to create a linear structure of eddy currents in a particular part of their distribution across a significant area of the TO surface, thanks to their elongated shape. This is achieved using long parallel conductors that form an almost uniform field between them, which is impossible with circular alternative coil configurations, or by a special numerical procedure for synthesizing the electromagnetic field [26–29].

The excitation coil is placed parallel to the plane of the TO, while the pick-up coil is orthogonal to it. The TO is represented by two layers. The first of them, with a thickness of d_1 and an electrical conductivity of σ_1, is associated with a metal nonmagnetic coating. The metal substrate of the TO is composed of a second layer of infinite thickness $d_2 = \infty$ and electrical conductivity σ_2, which is also nonferromagnetic. Thus, the magnetic properties of both layers of the TO are generally characterized by relative magnetic permeability $\mu_1 = 1$ and $\mu_2 = 1$, respectively. The TO is assumed to be of infinite width and length and moves with speed v along the Oy axis. It was created under the following assumptions: the TO medium is linear, isotropic, and homogeneous.

The rectangular excitation coil is characterized by geometric dimensions $2a_1 \times 2b_1$ and cross section $w_1 \times h_1$. It has the number of turns N_1. The coil is located at a height z_1 above the surface of the TO. The law of current variation of a multiturn excitation coil is sinusoidal $Ie^{j\omega t}$ with an angular frequency ω. The pick-up coil with dimensions $2a_2 \times 2b_2$ and height z_2 is characterized by a cross section $w_2 \times h_2$. It has N_2 turns. The coil is displaced from the Oz axis in the direction of the Ox axis by a distance c.

A mathematical model suitable for the above calculations of the ECP output signal was created and verified by the authors of the research [30]. It should be noted that it is adequate under the assumptions of linearity, isotropy, and homogeneity of the environments of the two-layer TO. The induced electromotive force (EMF) of the probe over the moving TO is calculated by the following

Table 2 A set of uncontrollable parameters

Uncontrollable factor	Variation range	
Coating materials	Al	Cd
Electrical conductivity of the coating σ_1 (10^6 S/m)	34.92–37.08	13.58–14.42
Substrate materials	Steel 12X18H10T	Cu
Electrical conductivity of the substrate σ_2 (10^6 S/m)	1.296–1.404	55.68–60.32
Lift-off $z_1 = z_2 = z$, (10^{-3} m)	0.5–3	–

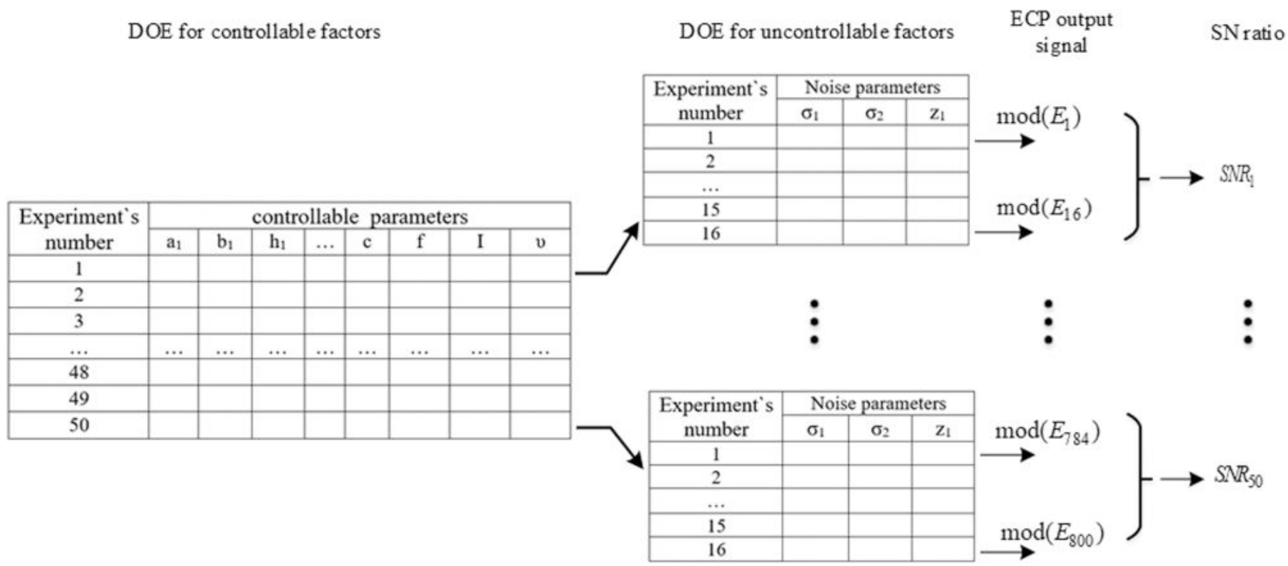

Fig. 2 Scheme for drawing up a Taguchi design of experiments

expression [30] with the relevant corrections from Ref. [31]:

$$E=\frac{2\omega\mu_0 IN_1N_2}{\pi^2 w_1h_1w_2h_2}\int_{-\infty}^{\infty}\int_{-\infty}^{\infty}\frac{\kappa k_1k_2}{\eta^2\xi\varsigma^2}\sin\left(\frac{h_2\xi}{2}\right)e^{-j\xi c}\times \times[e^{-(2z_1+w_2+a_2)\varsigma}-e^{-(2z_1+w_2+a_2+h_1)\varsigma}]d\xi d\eta \quad (1)$$

- where $\kappa=\dfrac{\left(\frac{\gamma_1}{\varsigma}-\frac{\mu_1}{\mu_0}\right)\cdot\left(\frac{\gamma_2}{\gamma_1}+\frac{\mu_2}{\mu_1}\right)+\left(\frac{\gamma_1}{\varsigma}+\frac{\mu_1}{\mu_0}\right)\cdot\left(\frac{\gamma_2}{\gamma_1}-\frac{\mu_2}{\mu_1}\right)\cdot e^{-2\gamma_1 d_1}}{\left(\frac{\gamma_1}{\varsigma}+\frac{\mu_1}{\mu_0}\right)\cdot\left(\frac{\gamma_2}{\gamma_1}+\frac{\mu_2}{\mu_1}\right)+\left(\frac{\gamma_1}{\varsigma}-\frac{\mu_1}{\mu_0}\right)\cdot\left(\frac{\gamma_2}{\gamma_1}-\frac{\mu_2}{\mu_1}\right)\cdot e^{-2\gamma_1 d_1}}$
- $k_1=\dfrac{\sin[a_1\xi-b_1\eta+(\xi-\eta)w_1]-\sin(a_1\xi-b_1\eta)}{2(\xi-\eta)}+ +\dfrac{\sin(a_1\xi+b_1\eta)-\sin[a_1\xi+b_1\eta+(\xi+\eta)w_1]}{2(\xi+\eta)}$
- $k_2=\dfrac{\varsigma\sin\eta(b_2+w_2)[e^{\varsigma(w_2+a_2)}+e^{-\varsigma(w_2+a_2)}]-\eta\cos\eta(b_2+w_2)[e^{\varsigma(w_2+a_2)}+e^{-\varsigma(w_2+a_2)}]}{\eta^2+\varsigma^2}+ +\dfrac{\eta\cos(\eta b_2)[e^{\varsigma a_2}-e^{-\varsigma a_2}]-\varsigma\sin(\eta b_2)[e^{\varsigma a_2}+e^{-\varsigma a_2}]}{\eta^2+\varsigma^2}$
- $\gamma_1=\sqrt{\xi^2+\eta^2-j\sigma_1\mu_1\nu\eta+j\omega\sigma_1\mu_1}$
- $\gamma_2=\sqrt{\xi^2+\eta^2-j\sigma_2\mu_2\nu\eta+j\omega\sigma_2\mu_2}$
- $\varsigma=\sqrt{\xi^2+\eta^2}$
- ξ and η are the integration variables of the Fourier transform
- $\mu_0=4\cdots\pi\cdots10^{-7}$ H/m is the magnetic constant in a vacuum

The calculations must take into account certain subtleties inherent in the calculation of eddy current thickness gauges during design. During electromagnetic field sensing of nonmagnetic metal coatings applied to a nonferromagnetic metal substrate of the TO, in general, the induced signal of the probe is formed under the influence of certain contributions, one of which is due to the substrate material and the other due to the coating material. The contribution of these components to the value of the ECP signal varies depending on the excitation frequency. Also, the changes in the contribution value are affected by the thickness of the conductive layers of the TO and the situation with the depth sequence of better or worse conductivity of the layers. The thickness of the coating can be estimated if both materials have sufficiently different electrophysical properties, in particular, the multiplication of conductivity and permeability $(\sigma_1\cdot\mu_1)$ for one of the materials should be at least 1.5 times greater than the multiplication of conductivity and permeability $(\sigma_2\cdot\mu_2)$ for the other material [32]. For measurements of coatings on a metal substrate, the total thickness of the conductive materials of the substrate and the coating should be at least three standard depths of penetration into the TO of eddy currents [32]. The classical, well-known formula calculates the standard depth of the penetration of eddy currents.

2.3 Taguchi Design of Experiments and Optimal Design. Under the algorithm for performing robust parameter design of eddy current thickness gauges of coatings, we will determine the choice of sets of controllable and uncontrollable parameters, which are given in Tables 1 and 2. The tables also indicate the selected ranges of changes in the parameters affecting the probe signal.

Two types of TO structures are considered, in particular, the first of them is Al–steel (structure 1) on a weakly magnetic substrate, and the second is Cd–Cu (structure 2) on a nonmagnetic substrate, respectively, whose conducting properties of the materials are presented in Table 2.

So, we have 12 controllable parameters and three uncontrollable ones. In further experiments, the controllable parameters will be

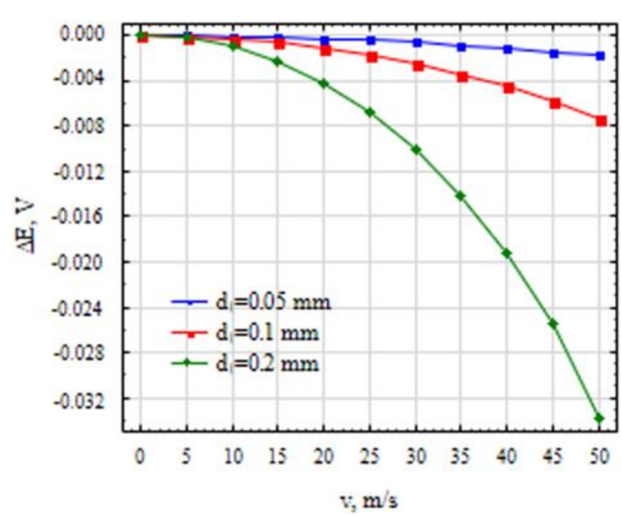

Fig. 3 Results of verification calculations of differences in the amplitudes of induced EMFs at varying speeds of the TO movement for different coating thicknesses

Table 3 Design of experiment for controllable parameters

No.	a_1 (10^{-3} m)	b_1 (10^{-3} m)	h_1 (10^{-3} m)	w_1 (10^{-3} m)	a_2 (10^{-3} m)	b_2 (10^{-3} m)	h_2 (10^{-3} m)	w_2 (10^{-3} m)	c (10^{-3} m)	f (kHz)	I (A)	v (m/s)
1	17.5	16	4	1.00	3.0	10	1.00	1.00	2.00	1.50	0.1	15.0
2	17.5	18	5	1.75	3.5	11	1.25	1.25	3.75	2.25	0.1	17.5
3	17.5	20	6	2.50	4.0	12	1.50	1.50	5.50	3.00	0.1	20.0
4	17.5	22	7	3.25	4.5	13	1.75	1.75	7.25	3.75	0.1	22.5
5	17.5	24	8	4.00	5.0	14	2.00	2.00	9.00	4.50	0.1	25.0
…	…	…	…	…	…	…	…	…	…	…	…	…
27	10.0	18	5	4.00	3.0	14	1.75	1.50	2.00	3.00	0.3	22.5
28	10.0	20	6	1.00	3.5	10	2.00	1.75	3.75	3.75	0.3	25.0
29	10.0	22	7	1.75	4.0	11	1.00	2.00	5.50	4.50	0.3	15.0
30	10.0	24	8	2.50	4.5	12	1.25	1.00	7.25	1.50	0.3	17.5
31	12.5	16	5	1.00	4.0	12	1.25	1.75	9.00	4.50	0.3	22.5
…	…	…	…	…	…	…	…	…	…	…	…	…
47	20.0	18	4	2.50	4.0	10	1.75	2.00	9.00	3.75	0.3	17.5
48	20.0	20	5	3.25	4.5	11	2.00	1.00	2.00	4.50	0.3	20.0
49	20.0	22	6	4.00	5.0	12	1.00	1.25	3.75	1.50	0.3	22.5
50	20.0	24	7	1.00	3.0	13	1.25	1.50	5.50	2.25	0.3	25.0

Table 4 Design of experiment for interfering parameter structure 1

Experiment	1	2	3	4	5	…	14	15	16
σ_1 (10^6 S/m)	34.92	35.64	36.36	37.08	35.64	…	36.36	35.64	34.92
σ_2 (10^6 S/m)	1.296	1.332	1.368	1.404	1.368	…	1.296	1.404	1.368
z_1 (10^{-3} m)	0.50	1.33	2.16	3.00	3.00	…	3.00	0.50	1.33

Table 5 Design of experiment for interfering parameter structure 2

Experiment	1	2	3	4	5	…	14	15	16
σ_1 (10^6 S/m)	13.58	13.86	14.14	14.42	13.86	…	14.14	13.86	13.58
σ_2 (10^6 S/m)	55.68	57.23	58.77	60.32	58.77	…	55.68	60.32	58.77
z_1 (10^{-3} m)	0.50	1.33	2.16	3.00	3.00	…	3.00	0.50	1.33

considered at five levels of gradation, and the uncontrollable parameters will be considered at four levels of gradation, respectively. Based on considerations of the number of parameters in the two groups and their gradation levels, we choose orthogonal arrays $L_{50}(2^1, 5^{11})$ and $L_{16}(4^5)$ [33,34]. The first of them involves 50 observations, and it was created for 11 factors at five grading levels and one factor at two levels, respectively. It was decided that the operating controllable parameter, namely, the excitation current I, would be considered at two levels of gradation, and all others at five. In other words, the factors have been ordered according to the template of the selected orthogonal array $L_{50}(2^1, 5^{11})$. The second array determines the execution of 16 experiments for five factors at four levels of gradation. So, we have two unnecessary factors in it, which, thanks to the properties of orthogonal arrays, can be removed by simply removing two columns from the standard array. Information on how to fill arrays with data can be found in the literature on this issue, including the one mentioned earlier in this article. For reasons of cumbersomeness, the arrays themselves are not presented in numerical form in these studies. Taguchi's-DOE, taking into account the previously presented information, is drawn up in accordance with the scheme illustrated in Fig. 2.

The scheme involves the calculation of specific SNR indicators introduced by Taguchi based on computer modeling data in accordance with the established observation design, which is performed taking into account the "larger is better" property according to formula (2) using the quality loss function:

$$\mathrm{SNR} = -10 \cdot \lg\left(\frac{1}{n} \cdot \sum_{i=1}^{n} \frac{1}{\mathrm{mod}(E_i)^2}\right) \quad (2)$$

- where $\mathrm{mod}(E_i)$ is the module of the output signal of a particular type of probe design under the action of the ith noise combination;
- n is the number of noise combinations.

The SNR ratio is an indicator of the measurement process efficiency, which combines the average measured signal and variance. Therefore, expression (2) is subject to maximization, and its result is a compromise between setting the output signal of the gauge at the desired maximum target level and keeping its variance at a low level. The indicator is calculated based on the probe responses to the data set contained in the DOE table. The variant of the ECP design is considered to be better the higher the SNR and the smaller the deviation of the ECP output signal from the target value, i.e., the smaller the variations. Such estimates allow us to make conclusions about the best values of the controllable parameters selected on their discretized set. That is, the problem of finding Taguchi's parameters is solved, which in combination determines the optimal design of the probe, which provides the maximum SNR and at the same time the minimum possible variation of the output signal under the condition of interference within the research ranges of their changes. A confirmation experiment to determine the SNR for the optimal design of the ECP and its comparison with similar factors of the analyzed design options allows us to verify the correctness of the technical decision.

2.4 ANOVA Variance Analysis. The variance ANOVA analysis is the final stage of research aimed at establishing the hierarchy of factor influence of the controllable parameters on the ECP signal, which is crucial for formulating technical requirements for the manufacture of the structure.

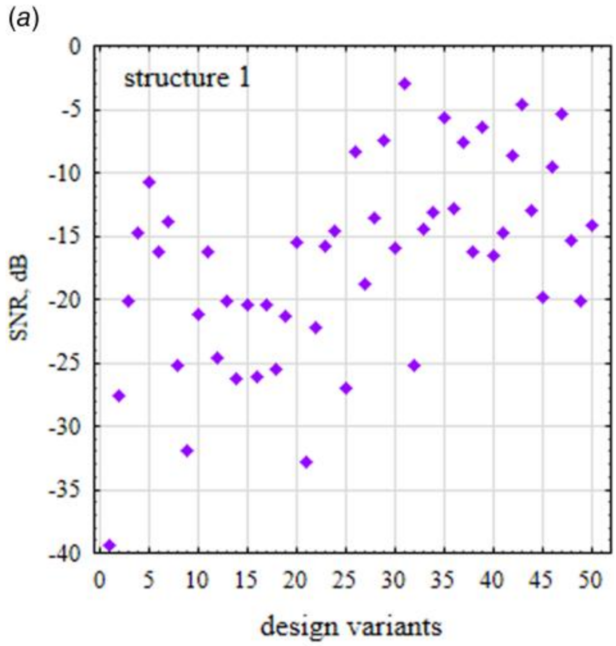

Fig. 4 (*a*) and (*b*) SNR values for all studied ECP design variants for both analyzed TO structures

The hierarchical of influence design parameters on the SNR is assessed by variance according to Fisher's criterion, based on statistical indicators such as *MS*—mean square of the variance component, MS_{residual}—mean square of the residuals, m_1—number of degrees-of-freedom for the corresponding factor, and m_2—number of degrees-of-freedom of residuals. The validity of the assumptions for applying the criterion was previously checked [33–35]. The conclusion about the significance of the influence of a particular design parameter was made by checking the condition $MS/MS_{\text{residual}} > F_{\alpha,m_1,m_2}$, where α is the accepted significance level, F_{α,m_1,m_2} is the tabular value of Fisher's criterion for the accepted α and the number of degrees-of-freedom. If the condition is met, the influence of the factor is significant, and vice versa.

3 Results

Although the mathematical model (1) is obtained in an analytical form, it requires the use of computer calculations. For this purpose, the corresponding software was created, the adequacy of which was proved by testing on the model examples given in Ref. [30]. Verification numerical calculations were performed with the following design parameters of the excitation coil: $a_1 = 12$ mm, $b_1 = 12$ mm, $z_1 = 1$ mm, $w_1 = 2$ mm, $h_1 = 8$ mm, $N_1 = 500$, and the pick-up coil: $a_2 = 3$ mm, $b_2 = 5$ mm, $z_2 = 1$ mm, $w_2 = 5$ mm, $h_2 = 2$ mm, $c = 8$ mm, and $N_2 = 300$. The electrophysical parameters of the TO were set as follows: $\sigma_1 = 3.8 \cdots 10^7$ S/m, $\mu_1 = 1$, $\sigma_2 = 5.8 \cdots 10^7$ S/m, and $\mu_2 = 1$. Excitation frequency $f = 2$ kHz and current $I = 1$ A. The results of the modeling are shown in Fig. 3. It shows graphs of the differences in the amplitudes of the EMFs induced in the pick-up coil, obtained for a moving and a static TO at varying speeds and for different coating thicknesses. We can demonstrate that the patterns in the analyzed distributions are properly observed, and the coincidence of modeling results with the data is presented in Ref. [30].

Subsequently, the selected orthogonal arrays for controllable and uncontrollable factors were used for numerical modeling, for which DOE output data in units of real physical quantities were obtained within the specified variation limits. Since the controllable design parameters are the same for both structures under study, the DOEs for them are identical, and their general form is shown in Table 3. The situation with interfering factors is another. Therefore, the DOE elements for the interfering uncontrollable parameters of structure 1 are presented in Table 4, and for structure 2 in Table 5. In addition, to make the experiments according to Taguchi's design for determining the probes' EMF using the mathematical model (1), the following values of relative magnetic permeability were set: for structure 1, $\mu_1 = 1$ and $\mu_2 = 1.3$; for structure 2, $\mu_1 = 1$ and $\mu_2 = 1$. Thus, with such initial data, the possibility of measuring the thickness of coatings applied not only to a nonmagnetic but also to a weakly magnetic substrate was investigated. This consideration of the materials of structure 1 was performed in order to expand the application of the eddy current method. Taking into account the standard depth of penetration of the electromagnetic field, the thickness of the coating was assumed to be $d_1 = 0.5$ mm. As a result, for each of the 50 experiments with 16 different variations of the influence of uncontrollable noise parameters, the values of the EMFs of the probes *E*, *V* were obtained.

In order to determine the optimal controllable parameters of the ECP, taking into account the "larger is better" property, we have previously calculated the values of signal-to-noise ratios for each of the designed experiments for both structures, the results of which are shown in Figs. 4(*a*) and 4(*b*), respectively. To do this, a number of statistical indicators were determined for each controllable parameter at all levels of its gradations [20,22], based on which the optimal probe parameters are found that provide the maximum available SNR. As a result, we found the optimal design of the ECP for each of the researched structures. The

Table 6 The design and operating parameters of optimal ECP design variant

Taguchi-parameters	a_1 (10^{-3} m)	b_1 (10^{-3} m)	h_1 (10^{-3} m)	w_1 (10^{-3} m)	a_2 (10^{-3} m)	b_2 (10^{-3} m)	h_2 (10^{-3} m)	w_2 (10^{-3} m)	c (10^{-3} m)	f (kHz)	I (A)	v (m/s)
Values	15	24	4	4	5	14	1.75	2	9	4.5	0.3	17.5

design and operating parameters of the optimal design for structure 1 are shown in Table 6.

It should be noted that similar design parameters were obtained for structure 2. Optimal probe designs provide SNR values of 1.76 dB for structure 1 of material 1 and 0.86 dB for structure 2.

In order to make sure that the found optimal designs provide not only the highest possible values of SNR but also that the output signals have reduced variations around their non-noise cases, the effect of various noises on their signals was studied by the Monte-Carlo method. That is, in this research, we set the optimal parameters of the ECP, borrowed from Table 6, and calculated their output signals when they are exposed to noise parameters, both individually and in combination. These noise factors were the electrical conductivity of the coating σ_1, the lift-off z_1, and the electrical conductivity of the substrate σ_2. They varied according to a uniform distribution law within $\pm 5\%$ of their constant values (structure 1: $\sigma_1 = 36 \cdots 10^6$ S/m, $\sigma_2 = 1.35 \cdots 10^6$ S/m; structure 2: $\sigma_1 = 14 \cdots 10^6$ S/m, $\sigma_2 = 58 \cdots 10^6$ S/m). The number of computer experiments was 25 realizations. For comparison, similar researches were performed for the best nonoptimal design no. 31, selected from Table 3, for which the SNR levels are the highest and amount to −2.973 and −3.824 dB for both tested TO structures (Fig. 4).

Then, for the first in a series of experiments, when a random change σ_1 acts on the probe, ECP signals were obtained for both structures, the values of which are shown in Figs. 5(*a*) and 5(*c*) for optimal designs and in Figs. 5(*b*) and 5(*d*) for nonoptimal ones. In addition, here and in the following figures, the maximum relative deviation $\delta_{\max}$, % of the ECP signal from its non-noise case is additionally indicated.

Figures 6(*a*) and 6(*b*) demonstrate for structure 1 the dependences of the output signals of the probes of the optimized and non-optimized designs on the change in the lift-off z_1, which varied from 0.5 mm to 3 mm with the same uniform distribution. Similar graphs, but for structure 2, are shown in Figs. 6(*c*) and 6(*d*).

By setting the change in the electrical conductivity of the substrate σ_2 as a noise factor, the following corresponding dependences of the output signals of the probes for the variants of the optimal (Figs. 7(*a*) and 7(*c*)) and nonoptimal (Figs. 7(*b*) and 7(*d*)) designs were obtained. And, finally, a research on the

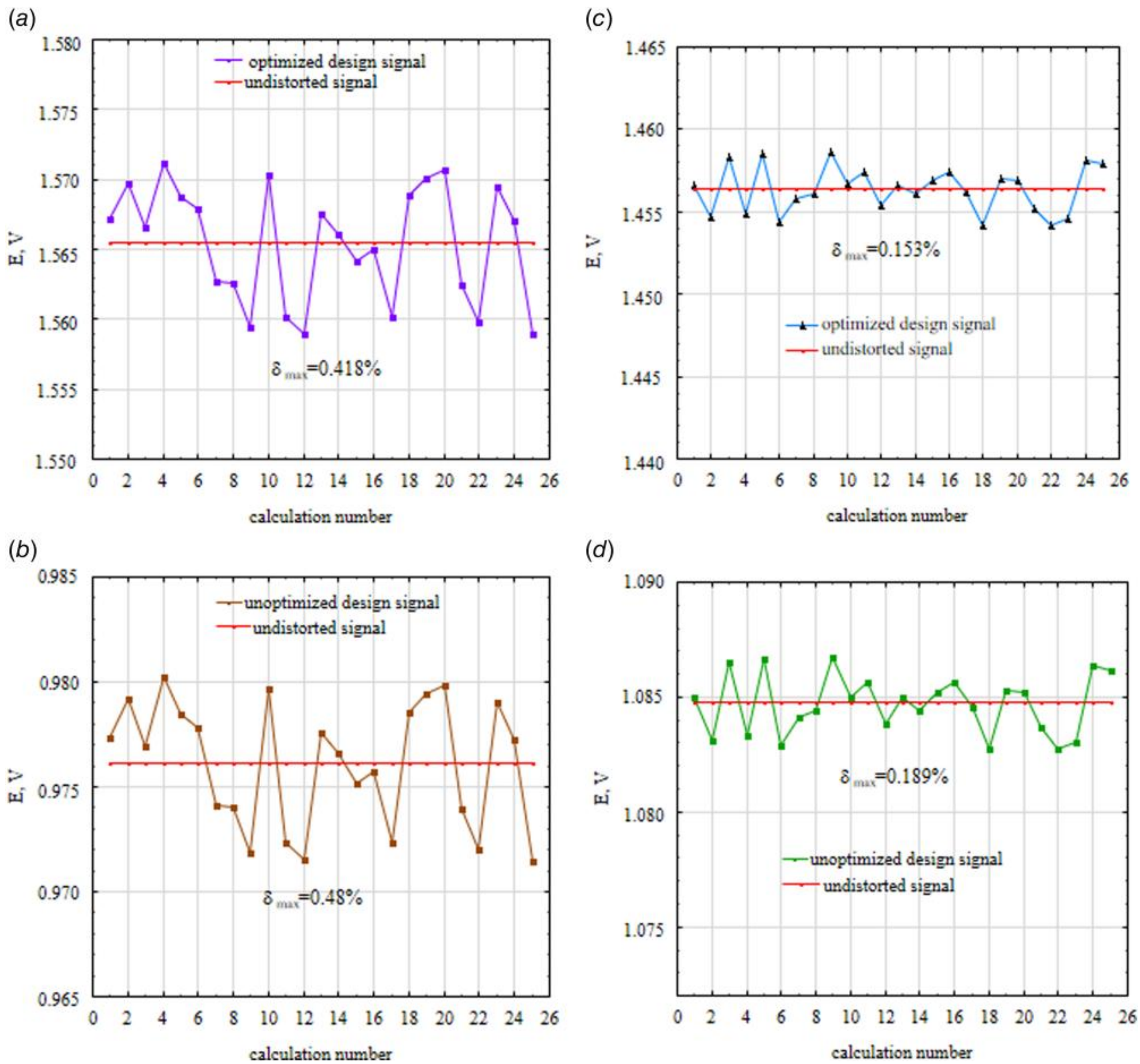

Fig. 5 (*a*)–(*d*) Influence of variations in the electrical conductivity of the coating σ_1 on the signal: (*a*) and (*b*) for material structure 1; (*c*) and (*d*) for material structure 2

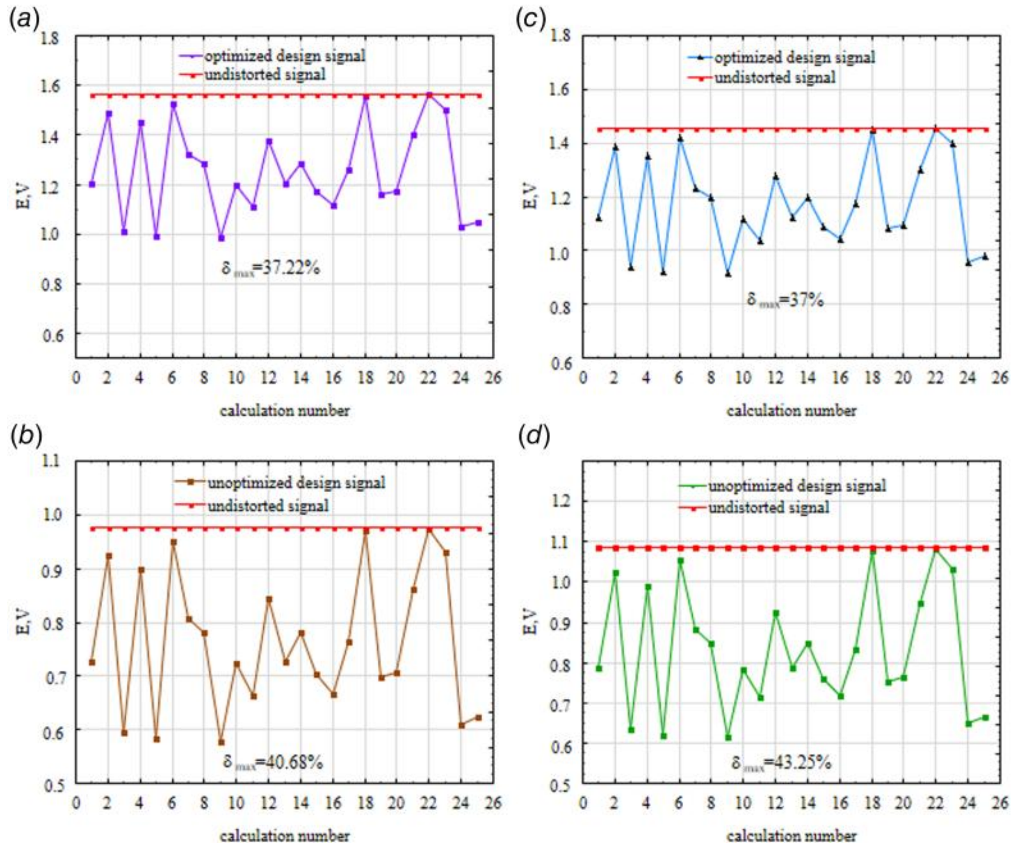

Fig. 6 (*a*)–(*d*) Influence of lift-off variations z_1 on the signal: (*a*) and (*b*) for material structure 1; (*c*) and (*d*) for material structure 2

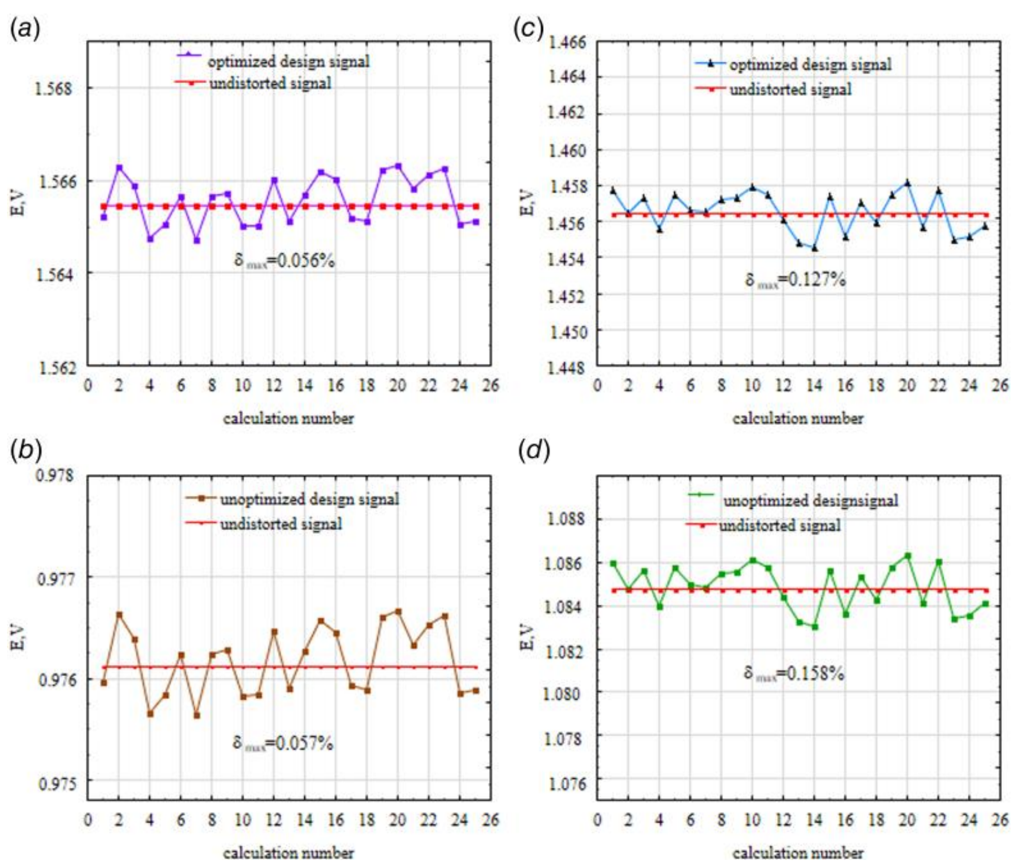

Fig. 7 (*a*)–(*d*) Influence of variations in the electrical conductivity of the substrate σ_2 on the signal: (*a*) and (*b*) for material structure 1; (*c*) and (*d*) for material structure 2

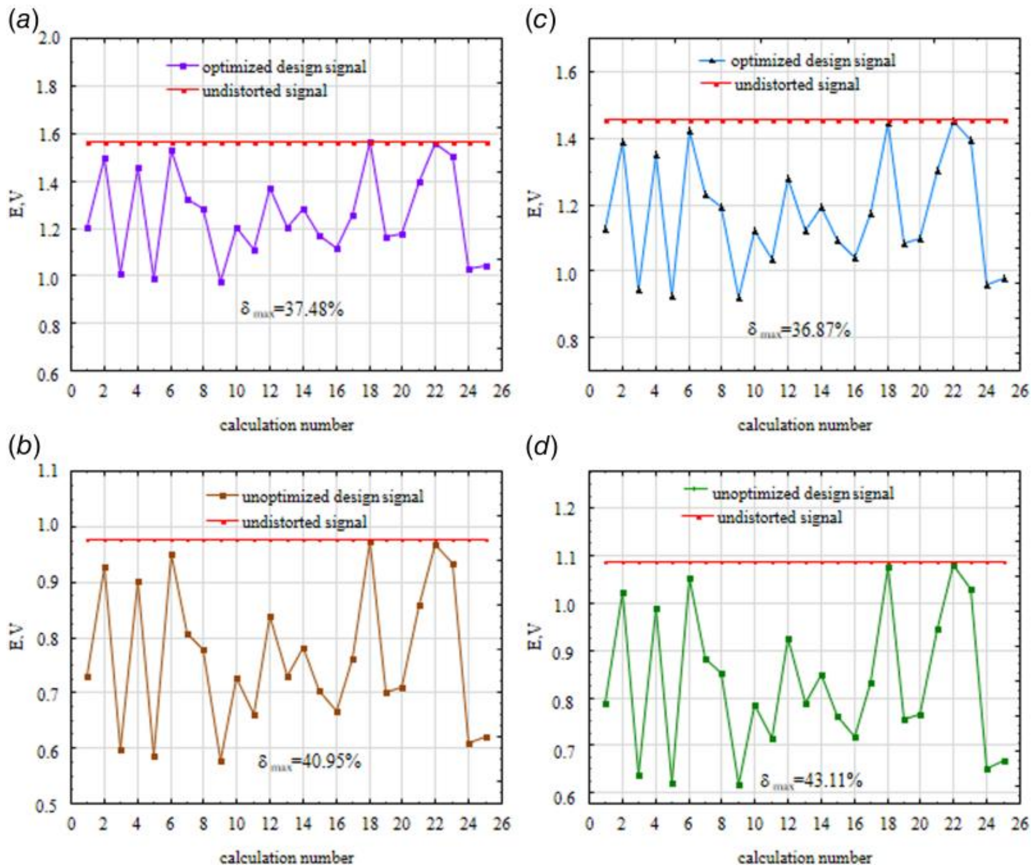

Fig. 8 (*a*)–(*d*) Influence of variations in the combination of all noise factors simultaneously on the signal: (*a*) and (*b*) for material structure 1; (*c*) and (*d*) for material structure 2

simultaneous influence of all these noise factors on the output signals of the ECP was carried out, and the results of which are shown in Figs. 8(*a*) and 8(*b*) for structure 1 and in Figs. 8(*c*) and 8(*d*) for the other.

For both material TO structures, in the case of the simultaneous action of a set of noise factors, for each of the 25 combinations, the values of the relative deviations δ, % of the probe signals from the non-noise variant were obtained, as illustrated in Fig. 9.

Although the best nonoptimized design shows only minor degradation in performance compared to the optimal design, other nonoptimized designs show significant degradation. Figure 10 demonstrates this for the worst nonoptimized probe design numbered 1 for material structure 1. This design corresponds to both material structures in terms of the lowest SNR values. Similar experimental results were obtained for material structure 2, so they are not shown.

With the previously stated aim, a variance analysis of the data was also conducted. The accepted significance level α for Fisher's criterion was 5%. The tabular values of Fisher's criterion for both structures are the same, since the experimental conditions are not different. For example, for the controllable operating parameter, the excitation current, for which $m_1 = 1$, this value is $F_{0.05,1,4} = 7.709$, and for all other parameters, it is $F_{0.05,4,4} = 6.388$, when $m_1 = 4$ and $m_2 = 4$. As a result, it was found that only the controllable parameters w_1, h_2 and speed v do not have a statistically significant effect on the SNR for both variants of structures. Thus, for structure 1, the ratio MS/MS_{residual} for the design parameter w_1 is 1.51, and for h_2 it is 0.95 and 0.41 for the velocity parameter v, which is less than the table value $F_{0.05,4,4}$, i.e., the effect is statistically insignificant. For all other parameters, this condition is met, so these factors are statistically significant. A similar situation is observed for structure 2. Tables 7 and 8 are provided below, where SS denotes the sum of squares of deviations from the mean for each factor, and F denotes the experimental values of Fisher's test.

An analysis of the data in Tables 7 and 8 has established a hierarchy of the effects of design parameters on the SNR. Thus, the ranking order of the most influential to the least influential design parameters of the probes is as follows: the center-to-center distance between the pick-up and excitation coils c, the length of the pick-up coil b_2, the width of the pick-up coil a_2, the height of the excitation coil cross section h_1, the length of the excitation coil b_1, the width of the excitation coil a_1, and the width of the pick-up coil cross section w_2. Numerical experiments were conducted to investigate the effect on the SNR of the manufacturing accuracy of ECP designs, that is, deviation from their parameters by up to ± 0.5 mm was permissible. The results show that, in the worst-case scenario, these changes in geometric dimensions result in a decrease in SNR of 0.413 dB for structure 1 and 0.42 dB for structure 2, compared to their optimal values of 1.76 dB and 0.86 dB.

4 Discussion

Thus, as a result of numerous experiments, it has been established that the optimal probe designs provide the maximum possible SNR value. For structure 1 of the material, this value is 1.76 dB, and for structure 2, it is 0.86 dB, which is greater than any SNR value for nonoptimized design options (Fig. 4) given in Taguchi's design of experiments.

Then, the increment of SNR (ΔSNR) was defined as the absolute difference between its maximum (minimum) value for the poorest and the best of the nonoptimized designs and the corresponding value of the optimal design. Thus, for structure 1 of the material, the maximum increment is $\Delta \text{SNR}_{max} = 41.09$ dB, and the

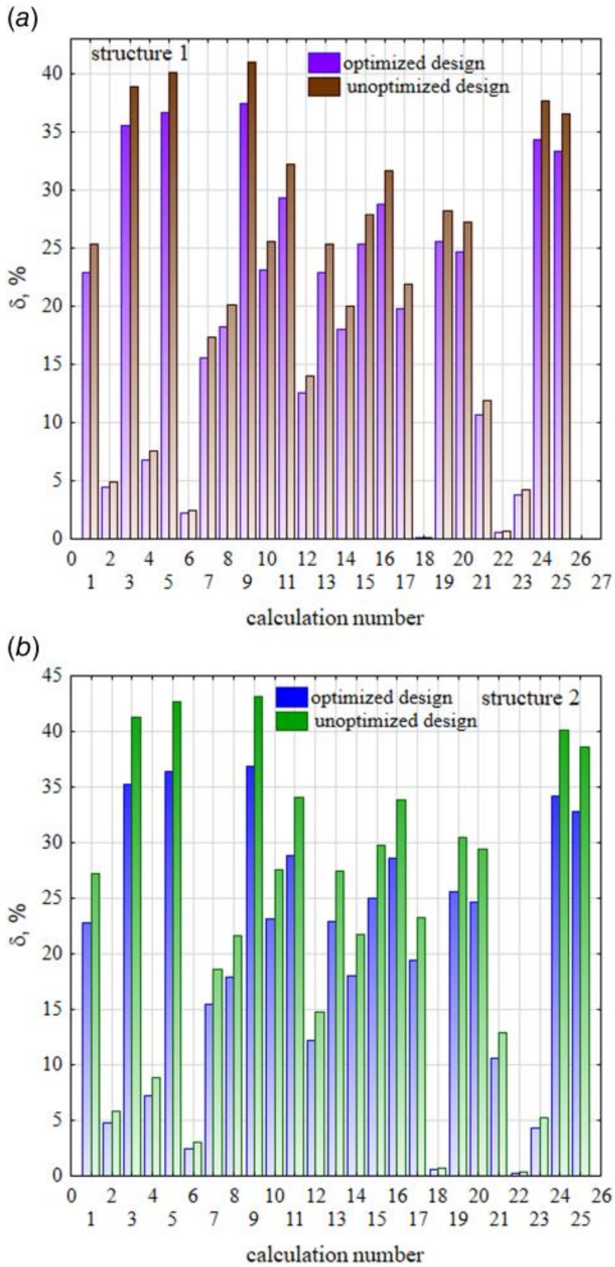

Fig. 9 (*a*) and (*b*) Values of relative deviations δ, % of ECP signals from the noiseless one under the simultaneous action of the set of variations of all noise factors: (*a*) structure 1 and (*b*) structure 2

minimum is $\Delta SNR_{min} = 4.73$ dB, respectively. And for structure 2, $\Delta SNR_{max} = 39.85$ dB and $\Delta SNR_{min} = 4.68$ dB. Even at its minimum value, this increment results in an increase in the probe signal level of approximately 72.6% and 69.5% relative to the average for the designs of both structures, respectively, demonstrating the significant practical importance of the proposed method for designing ECPs.

There is also a decrease in the variations of the output signals of the probes for their optimal designs in all cases of various noise factors, as demonstrated in Figs. 5–9 for both structures under study.

Thus, with a variation in the electrical conductivity of the coating σ_1, the maximum relative deviation δ_{max},% of the ECP signal from its undistorted case for optimized designs is 0.418% for structure 1 and 0.153% for structure 2, which is better than the best nonoptimized design options, for which it is 0.48% and

Table 7 Variance analysis indicators for material structure 1

Parameters	*SS*	*m*	*MS*	*F*	*p*	*Q* (%)
a_1	8.043	4	2.011	64.12	0.0007	0.13
b_1	9.198	4	2.300	73.33	0.0005	0.14
h_1	14.26	4	3.564	113.6	0.0002	0.22
w_1	0.189	4	0.047	1.510	0.3507	0.01
a_2	31.75	4	7.937	253.1	0.0001	0.50
b_2	37.21	4	9.303	296.6	0.0001	0.58
h_2	0.119	4	0.030	0.950	0.5193	0.01
w_2	1.635	4	0.409	13.04	0.0145	0.03
c	946.9	4	236.4	7541	0.0001	14.7
f	803.1	4	200.7	6402	0.0001	12.5
v	0.050	4	0.013	0.410	0.7953	0.01
I	1146	1	1146	36,557	0.0001	71.2
residual	0.125	4	0.031	–	–	–

Note: p is the probability that the influence of the factor on the outcome variable is random, and Q is the percentage contribution of each factor to the total variance.

0.189%, respectively. In the case of variations in the lift-off z_1 as a noise factor, the results in Fig. 6 also show better values of the specified deviation for the optimized design options of both structures. These deviations amount to 37.22% for structure 1 and 37% for structure 2, which is 3.46% and 6.25% less, respectively, than the similar characteristics of the best nonoptimized designs.

The results obtained when the noise factor was set to the electrical conductivity of the substrate σ_2 (Fig. 7) are no exception, i.e., an insignificant improvement in δ_{max} is observed for both structures compared to the best nonoptimized designs. The same trend remains for the case when the probe is affected by a combination of variations of all noise factors simultaneously. Here, the relative deviation δ (Figs. 8(*a*) and 8(*c*)) ranges from 0.155% to 37.48% for materials of both structures, which is ensured by optimal designs. Accordingly, the best nonoptimized probe options δ (Figs. 8(*b*) and 8(*d*)) range from 0.167% to 43.11%. That is, the δ_{max} indicator for the optimized design options is better than this indicator for the best nonoptimized options by 3.47% and 6.24%, respectively. Thus, in all cases, there is a consistent pattern of reduction in the variations of the output signals for the optimized design variants of both structures of the studied materials. For the worst nonoptimized design option, even greater values of maximum relative deviations (Fig. 10) are observed compared to the optimal design of the meter (Figs. 5(*a*), 6(*a*), 7(*a*), and 8(*a*)).

It should be noted that the computational costs of the proposed method occur at the design stage, which is important for the use of real-time meters. Therefore, the method does not require signal processing, i.e., it does not affect the speed of measurements. Signals improved in this way at the formation stage can be further

Table 8 Variance analysis indicators for material structure 2

Parameters	*SS*	*m*	*MS*	*F*	*p*	*Q* (%)
a_1	7.809	4	1.952	97.450	0.0003	0.12
b_1	9.342	4	2.336	116.58	0.0002	0.15
h_1	14.10	4	3.522	175.81	0.0001	0.23
w_1	0.201	4	0.050	2.5000	0.1979	0.01
a_2	31.44	4	7.861	392.37	0.0001	0.50
b_2	36.80	4	9.198	459.11	0.0001	0.59
h_2	0.113	4	0.028	1.4200	0.3721	0.01
w_2	1.575	4	0.394	19.660	0.0068	0.03
c	941.3	4	235.3	11,746	0.0001	15.0
f	660.0	4	165.0	8236.4	0.0001	10.5
v	0.035	4	0.009	0.4400	0.7780	0.01
I	1142	1	1142	57,051	0.0001	72.9
Residual	0.080	4	0.020	–	–	–

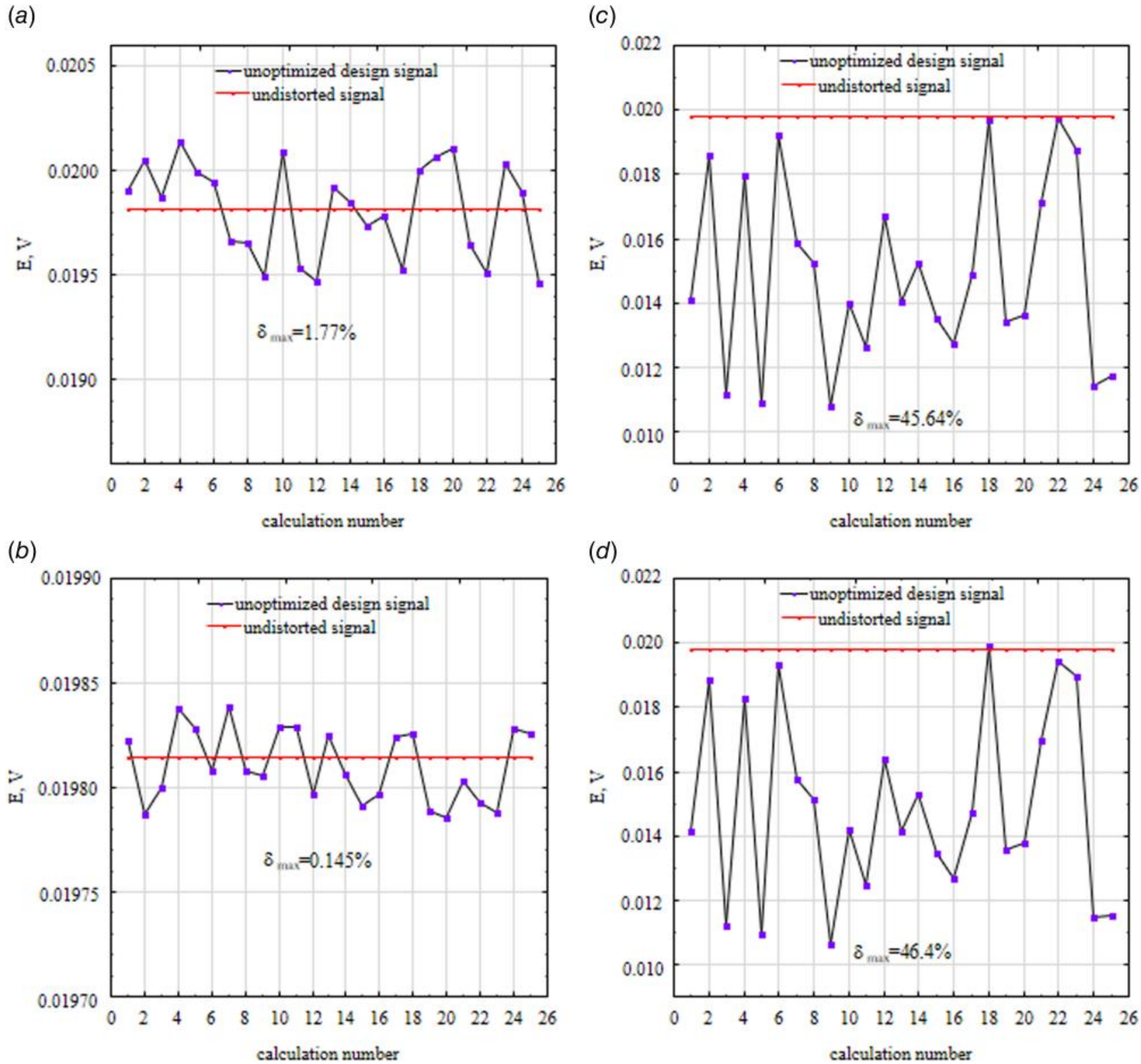

Fig. 10 (*a*)–(*d*) Influence of noise factors on the signal of the worst-case nonoptimized ECP design for material structure 1: (*a*) due to variations in the electrical conductivity of the coating σ_1, (*b*) due to variations in the lift-off z_1, (*c*) due to variations in the electrical conductivity of the substrate σ_2, and (*d*) due to the combination of variations in all noise factors simultaneously

processed in combination with the methods mentioned in the literature review.

5 Conclusions

The article extends and adapts the method previously created by the authors for improving SNR using Taguchi's robust parameter design to the entire class of surface transformer eddy current meters for nonmagnetic metal coatings applied to metal nonferromagnetic and weakly magnetic substrates of moved objects. The characteristic features of measuring the thickness of coatings on tested objects are taken into account, in particular, those caused by the need to simultaneously suppress all noise caused by local variations in the electrical conductivity of the coating materials and the substrate of the objects, as well as lift-off, even in the signal generation phase. That is, ensuring the insensitivity of meters to harmful and uncontrollable factors does not require signal processing after their selection.

The method is implemented using robust parameter design techniques based on the Taguchi method for finding the optimal configuration of probe designs. The designs of the experiments were created by modeling using an adequate and verified mathematical model of the measurement process and orthogonal arrays with high values of the gradation levels of influential factors, namely $L_{50}(2^1, 5^{11})$ and $L_{16}(4^5)$, which provide improved conditions for the effective search for optimal ECP designs due to the appropriate degree of discretization. The demonstration of the method's application is performed using the example of a surface eddy current probe with rectangular orthogonal coils, but it is possible for any design.

As a result of numerical computer experiments conducted for two types of TO structures, namely Al–steel and Cd–Cu, i.e., on weakly magnetic and nonmagnetic substrates, the optimal design and operating parameters of eddy current probes that ensure the specified properties in the studies have been determined. The minimum increment SNR is 4.73 dB and 4.68 dB for structures with nonmagnetic and weakly magnetic substrates, respectively.

In other cases, even better results are observed. The maximum increase is 41.09 dB and 39.85 dB, respectively, for the specified TO material structures.

The reliable effectiveness of the founded optimal configurations of ECP designs is illustrated by comparison with the SNR values for nonoptimal configurations. In addition, the numerical–experimental Monte-Carlo method has proven a significant reduction in the impact of various types of noise on the signals of optimal designs with an evaluation of variations around their undistorted noise variants. The improvements achieved are a maximum of 3.47% for material structure 1 and 6.25% for structure 2. However, finding a meter design that is similar in performance to the optimal one without using the proposed method requires significant calculations and time to select acceptable options, but does not guarantee a positive result.

Based on a number of statistical indicators, the hierarchical influence of design parameters on the SNR coefficient was evaluated using ANOVA according to Fisher's criterion. As a result, it was established that only the controllable parameters w_1, h_2 and velocity v do not have a statistically significant effect on this index for both variants of material structures. Therefore, it has been established that during the manufacture and operation of probes, the greatest attention should be paid to the stability of the frequency and excitation current and the accuracy of the fabrication of the following design parameters, in particular, the center-to-center distance between the coil system, the length and width of the pick-up coil, which have a statistically significant impact on the SNR. Numerical experiments have shown that when manufacturing ECP designs with an accuracy of $\pm$0.5 mm for all parameters, the worst-case reduction in SNR is no more than 0.42 dB.

The following symbols are used in this article:

TO, test object;
ECP, eddy current probe;
SNR, signal-to-noise ratio;
SFEC, swept-frequency eddy current;
PEC, pulsed eddy current;
MEC, multifrequency eddy current;
AECC, apparent eddy current conductivity;
DOE, design of experiment;
ANOVA, analysis of variance;
EMF, electromotive force;
MS, mean square of the variance component;
SS, sum of squares of deviations from the mean.

Funding Data

- The work was performed free of charge with the support of the research work of Cherkasy State Technological University (Project # 0125U003384).

Conflict of Interest

There are no conflicts of interest.

Data Availability Statement

The datasets generated and supporting the findings of this article are obtainable from the corresponding author upon reasonable request.

References

[1] Ge, J., Xu, F., and Yusa, N., 2024, "Experimental Investigation of Low-Frequency and Pulsed Eddy Current Testing in Thickness Measurement," NDT E, **40**(11), pp. 1–19.

[2] Chen, W., and Wu, D., 2023, "Metal Film Thickness Measurement Using Phase Linearity Feature for Immunity to Lift-Off Effect," NDT E Int., **140**, p. 102965.

[3] Santos, A. C., Barrancos, A., Rosado, L. S., and Janeiro, F. M., 2022, "Low-Cost Multi-Frequency Eddy Current Coating Thickness Measurement System," International Young Engineers Forum (YEF-ECE), Caparica /Lisbon, Portugal, July 1, IEEE, pp. 7–11.

[4] Xu, J., Wu, J., Xin, W., and Ge, Z., 2020, "Measuring Ultrathin Metallic Coating Properties Using Swept-Frequency Eddy-Current Technique," IEEE Trans. Instrum. Meas., **69**(8), pp. 5772–5781.

[5] Wang, Z., and Yu, Y., 2018, "Thickness and Conductivity Measurement of Multilayered Electricity-Conducting Coating by Pulsed Eddy Current Technique: Experimental Investigation," IEEE Trans. Instrum. Meas., **68**(9), pp. 3166–3172.

[6] Wang, Y., Fan, M., Cao, B., Ye, B., and Wen, D., 2020, "Measurement of Coating Thickness Using Lift-Off Point of Intersection Features From Pulsed Eddy Current Signals," NDT E Int., **116**, p. 102333.

[7] Hachi, D., Benhadda, N., Zaoui, A., Abdelhadi, B., Lefkaier, I. K., and Helifa, B., 2024, "Numerical Investigation to Study the Influence of Thickness and Electrical Conductivity of Metal-Sheets on the LOI-Point of a PEC Sensor," NDT E, **39**(4), pp. 886–904.

[8] Huang, P., Peng, L., Wen, S., Li, S., and Huang, S., 2025, "A Novel Eddy Current Testing for Permeability Measurement Reducing Lift-Off and Tilt Angle Effect," NDT E, **41**(4), pp. 1–19.

[9] Ali, A., Asif, A., Tian, G. Y., Aziz, F., and Abdin, M. Z. U., 2023, "Directly-Digitized Pulsed Eddy Current Based Quantification of Aluminum Sheet Thickness," Meas. Sci. Technol., **34**(12), p. 125902.

[10] Yu, Y., Zhang, D., Lai, C., and Tian, G., 2017, "Quantitative Approach for Thickness and Conductivity Measurement of Monolayer Coating by Dual-Frequency Eddy Current Technique," IEEE Trans. Instrum. Meas., **66**(7), pp. 1874–1882.

[11] Zhang, D., Yu, Y., Lai, C., and Tian, G., 2016, "Thickness Measurement of Multi-Layer Conductive Coatings Using Multifrequency Eddy Current Techniques," NDT E, **31**(3), pp. 191–208.

[12] Syasko, V., and Polacek, A., 2014, "Electromagnetic Thickness Measurement of Coatings. Situation and Prospects," Proceedings of the 11th European Conference on Non-Destructive Testing (ECNDT 2014), Prague, Czech Republic, Oct. 6–10, pp. 6–11.

[13] Wang, D., Xu, J., Xin, W., Zhu, S., and Han, Y., 2024, "Thickness and Conductivity Measurement of Nonferromagnetic Metal Coating Using Apparent Eddy Current Conductivity," IEEE Trans. Instrum. Meas., **73**, p. 6007410.

[14] Aldbaisi, A., Abu-Nabah, B. A., Alkhader, M., and Jaradat, M. A., 2024, "Eddy Current Conductive Coating Layer Assessment on Conductive Substrate: A Machine Learning Approach," NDT E, **40**(11), pp. 5290–5319.

[15] Ansari, Z. A., Abu-Nabah, B. A., Alkhader, M., and Muhammed, A., 2020, "Experimental Evaluation of Nonmagnetic Metal Clad Thicknesses Over Nonmagnetic Metals Using Apparent Eddy Current Conductivity Spectroscopy," Measurement, **164**, p. 108053.

[16] Xu, J., Wu, J., Wan, B., Xin, W., and Ge, Z., 2020, "A Novel Approach for Metallic Coating Detection Through Analogizing Between Coil Impedance and Plane Wave Impedance," NDT E Int., **116**, p. 102308.

[17] Ansari, Z. A., Abu-Nabah, B. A., and Alkhader, M., 2018, "Single-Frequency Apparent Eddy Current Conductivity Assessment of Metallic Coating Thicknesses Over Nonmagnetic Metals," Int. J. Appl. Electromagn. Mech., **56**(4), pp. 533–547.

[18] Abu-Nabah, B. A., 2017, "Metallic Coating Thickness Assessment Over Nonmagnetic Metals Using Apparent Eddy Current Conductivity Spectroscopy," Int. J. Appl. Electromagn. Mech., **54**(1), pp. 77–91.

[19] Koshevoy, M., Zabolotnyi, O., Tsekhovskyi, M., Koshevaya, I., and Kostenko, O., 2020, "Research and Optimization of the Eddy Current Transducer of Dielectric Coatings' Thickness on Metal Surfaces of Products," Ukrainian Metrol. J., **2**(2), pp. 33–39.

[20] Halchenko, V. Y., Trembovetska, R., Tychkov, V., and Kovtun, V., 2026, "Robust Parameter Design of Eddy Current Meters for Electrical Conductivity of Materials and Products of Considerable Thickness," Measurement, **258**, p. 119218.

[21] Halchenko, V. Y., Trembovetska, R., Tychkov, V., and Kovtun, V., 2026, "Robust Parameter Design of Eddy Current Measuring Devices for Magnetic Permeability of a Moving Strip of Ferromagnetic Rolled Metal," J. Nondestruct. Eval., **45**(1), p. 12.

[22] Halchenko, V. Y., Trembovetska, R., and Tychkov, V., 2026, "Reducing Noise Levels in Eddy Current Measurements Using Self-Differential Probes of the Substrate Conductivity Under a Layer of Conductive Coating in Moved Objects," Sci. Rep., **16**, p. 14769.

[23] Krishnaiah, K., and Shahabudeen, P., 2012, *Applied Design of Experiments and Taguchi Methods*, PHI Learning Pvt. Ltd.

[24] Zhang, J., Du, H., Xue, D., and Gu, P., 2021, "Robust Design Approach to the Minimization of Functional Performance Variations of Products and Systems," Front. Mech. Eng., **16**(2), pp. 379–392.

[25] Almansoori, N., Aldulaijan, S., Althani, S., Hassan, N. M., Ndiaye, M., and Awad, M., 2021, "Manual Spray Painting Process Optimization Using Taguchi Robust Design," Int. J. Qual. Reliab. Manage., **38**(1), pp. 46–67.

[26] Halchenko, V. Y., Trembovetskaya, R. V., and Tychkov, V. V., 2020, "Surface Eddy Current Probes: Excitation Systems of the Optimal Electromagnetic Field," Devices Methods Meas., **11**(2), pp. 91–104.

[27] Halchenko, V. Y., Trembovetska, R. V., and Tychkov, V. V., 2021, "Surrogate Synthesis of Excitation Systems for Frame Tangential Eddy Current Probes," Arch. Electr. Eng., **70**(4), pp. 743–757.

[28] Halchenko, V. Y., Trembovetska, R., and Tychkov, V., 2021, "Surrogate Synthesis of Frame Eddy Current Probes With Uniform Sensitivity in the Testing Zone," Metrol. Meas. Syst., **28**(3), pp. 551–564.

[29] Trembovetska, R., Halchenko, V., and Tychkov, V., 2018, "Studying the Computational Resource Demands of Mathematical Models for Moving

Surface Eddy Current Probes for Synthesis Problems," Eastern-Eur. J. Enterprise Technol., **5**(5), pp. 39–46.

[30] Zhang, S., and Ida, N., 2016, "Calculation Model for the Induced Voltage in Rectangular Coils Above Conductive Plates," Facta Univ. Ser.: Electron. Energet., **30**(1), pp. 27–38.

[31] Tanaka, A., Takehira, N., and Toda, K., 1981, "Analysis of a Rectangular Coil Facing to Moving Sheet Conductor," Trans. Inst. Electr. Eng. Jpn., **101**(8), pp. 405–412.

[32] Udpa, S. S., and Moore, P. O., 2004, *Nondestructive Testing Handbook*, 3rd ed., Vol. 5, American Society for Nondestructive, Columbus, OH, p. 524.

[33] Montgomery, D. C., 2017, *Design and Analysis of Experiments*, 9th ed., John Wiley & Sons, Arizona State University, p. 196.

[34] Zaiontz, C, Website, *Real Statistics Using Excel*, C. Zaiontz, ed., Real Statistics Resources. https://realstatistics.com/design-of-experiments/taguchi-design-of-experiments/taguchi-3-level-designs

[35] Berk, K. N., and Carey, P., 2004, *Data Analysis With Microsoft Excel*, 3rd ed., Thomson Learning, Belmont, CA, p. 613.